

Effect of Vent Position on Temperature Inhomogeneity Inside Apple Storage Package: A Numerical Study



Harshad Raghuwanshi, K. R. Aharwal, and Narendra Gajbhiye

1 Introduction

Special attention is needed to retain the shelf life, freshness, and quality of the food produce in post-harvest handling. Among the various methods of post-harvest handling, pre-cooling is one of the methods to maintain the quality and freshness of the food produce [1]. Temperature management is one of the crucial factors in the post-harvest handling of food produce. In the pre-cooling process, the field heat is removed from the harvested produce which reduces the metabolism of the product, hence retarded the deterioration process during storage and transportation. Low-temperature treatment of food produce also reduces microbial growth, moisture loss, enzymatic activities, and ethylene production. The low cost and high efficiency of the forced air pre-cooling technique make it widely accepted. This technique uses a fan to force the cold air over the produce package. This cold air takes the heat from the food produce and leaves through the ventilation in the packaging system. The packaging used to store the food produce hinders the direct contact of cold air with the product. Also, the design of the packaging complicates the airflow distribution. Thus, optimization of the packaging design is a crucial area to be explored.

H. Raghuwanshi · K. R. Aharwal (✉) · N. Gajbhiye
Department of Mechanical Engineering, MANIT, Bhopal 462003, India
e-mail: kraharwal@gmail.com

H. Raghuwanshi
e-mail: info4harsh@gmail.com

N. Gajbhiye
e-mail: nlgajbhiye@manit.ac.in

2 Literature Review and Objective

Vent area, shape, size, position, and stacking arrangement are some crucial design factors in the designing of food produce packaging. Han et al. [2] experimentally and numerically observed the effect on cooling heterogeneity inside the package by increasing the number of vent holes in the existing package filled with apples. In another numerical study, by the same authors cooling profile was observed after increasing the layers of the apples from two to four in a single package with varying the shape of the vents [3]. Wang et al. [4] numerically investigated the commercial packaging of strawberries by varying the shape of the vents for cold air and observed their effect on cooling performance. Han et al. [5] found that increasing the air inflow rate of cold air beyond a limit results in high energy consumption, excessive moisture loss, and chilling injury. To minimize moisture loss, plastic liners and poly liners can be used. Gruyters et al. [6] compared the cooling performance of traditional corrugated boxes with reusable plastic crates (RPC). Authors found that the performance of the RPC is better than the corrugated boxes for cooling uniformity and energy usage but they observed that the higher air flow rates result in chilling injury.

Apart from the packaging design, the tray placed in between the layers of the food produce also influences the airflow distribution inside the package. Gong et al. [7] numerically investigated the effect of the tray size placed between the apple layers. The complex package structure associated with the tray and food produce stacking results in complications of airflow distribution. This results in the cooling heterogeneity inside the package and consequently lowers the effectiveness of pre-cooling of the product. Bishnoi et al. [8–10] performed several experimental investigations on the airflow distribution and cooling heterogeneity in a cold room filled with products.

In the past few years, several experimental and numerical investigations are performed for optimizing the storage conditions of the food produce. Many researchers work on the optimization of vent shape, size, area, and stacking arrangement. The present study is focused on the effect of the position of the vent holes on the existing packaging of the apples. A 3-D CFD model of the package filled with apples is investigated numerically to find the optimum vent location on the package.

3 Numerical Models

3.1 Computational Domain

In the present study, a package filled with apples is placed in a 2.45 m long duct. The dimensions of the package are 0.27 m × 0.2 m × 0.45 m with 0.006 m thickness are considered. Four circular vents of 0.02 m diameter are kept at both sides of package perpendicular to the airflow. The schematic diagram of the duct with the apple filled package is shown in Fig. 1. A total of 24 apples are stored in each package in two layers. Each layer consists of 12 apples with a baffle plate in between them. The

baffle plate material assumed to be same material as of package with a 0.003 m thickness. Numerical simulations are conducted for three different positions of the vents on the package. The dimensions of the package with three different package designs termed A1, A2, and A3 are shown in Fig. 2.

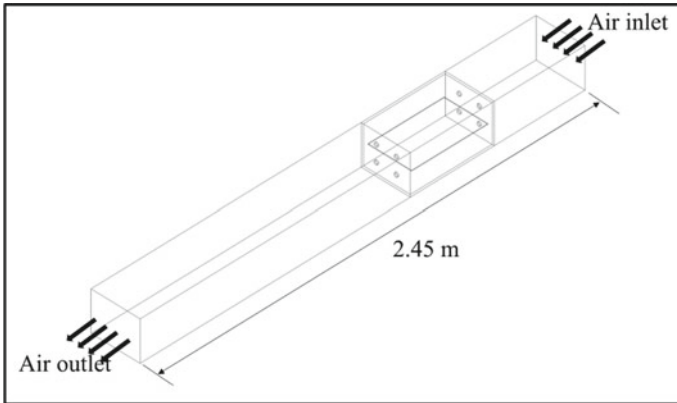


Fig. 1 Duct designed for the forced air pre-cooling with the package of apples

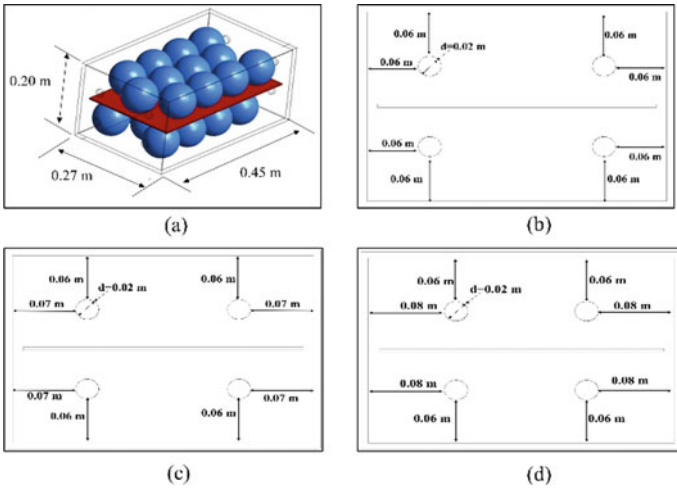


Fig. 2 a Dimensions of the package under study, b existing package design A1, c proposed package design A2, and d proposed package design A3

3.2 Governing Equations for Computational Domain

To solve the transient energy field and airflow in the computational domain, the Reynolds-averaged Navier Stokes (RANS) equations are used. The constant fluid properties are considered, and viscous heating is neglected in the present study. The governing equations used in the present study are as follows.

Conservation of Mass

$$\frac{\partial \rho_f}{\partial t} + \frac{\partial \bar{u}_i}{\partial x_i} = 0 \quad (1)$$

Conservation of Momentum

$$\rho_f \frac{\partial u_i}{\partial t} + \rho_f \frac{\partial \bar{u}_i \bar{u}_j}{\partial x_j} = -\frac{\partial \bar{P}_f}{\partial x_i} + \frac{\partial}{\partial x_j} \left[\nu \rho_f \left(\frac{\partial \bar{u}_i}{\partial x_j} + \frac{\partial \bar{u}_j}{\partial x_i} \right) \right] - \rho_f \frac{\partial \overline{u_i' u_j'}}{\partial x_j} \quad (2)$$

Conservation of Energy

$$\frac{\partial \bar{T}_f}{\partial t} + \bar{u}_i \left(\frac{\partial \bar{T}_f}{\partial x_i} + \frac{1}{\rho_f C_{P_f}} \frac{\partial \bar{P}_f}{\partial x_i} \right) = \frac{\partial}{\partial x_i} \left(\frac{\lambda_{\text{eff}}}{\rho_f C_{P_f}} \frac{\partial \bar{T}_f}{\partial x_i} \right) \quad (3)$$

The Reynolds stresses in Eq. (2) can be expressed based on Boussinesq hypothesis:

$$-\rho_f \overline{u_i' u_j'} = \nu_t \rho_f \left(\frac{\partial \bar{u}_i}{\partial x_j} + \frac{\partial \bar{u}_j}{\partial x_i} \right) - \frac{2}{3} \rho_f k \delta_{ij} \quad (4)$$

where ν_t is the kinematic eddy viscosity and k is the turbulence kinetic energy.

$$k = \frac{1}{2} \overline{u_i' u_i'} \quad (5)$$

Effective turbulent thermal conductivity λ_{eff} is expressed as

$$\lambda_{\text{eff}} = \lambda_f + \frac{C_{P_f} \nu_t \rho_f}{\text{Pr}_t} \quad (6)$$

Here, Pr_t is the turbulent Prandtl number and it is taken as 0.85.

Published study suggests that two equation eddy viscosity SST $k - \omega$ turbulence model gives better accuracy and convergence compared with other turbulence models (Standard $k - \varepsilon$, RNG $k - \varepsilon$, Standard $k - \omega$ turbulence model) [2, 7]. Hence, two equation eddy viscosity SST $k - \omega$ turbulence model is used in the present study with RANS equations. Following are the transport equations of SST $k - \omega$ turbulence model [11] that are used.

Turbulence Kinetic Energy

$$\frac{\partial k}{\partial t} + U_j \frac{\partial k}{\partial x_j} = P_k - \beta^* k \omega + \frac{\partial}{\partial x_j} \left[(v + \sigma_k v_T) \frac{\partial k}{\partial x_j} \right] \quad (7)$$

Specific Dissipate Rate

$$\frac{\partial \omega}{\partial t} + U_j \frac{\partial \omega}{\partial x_j} = \alpha S^2 - \beta \omega^2 + \frac{\partial}{\partial x_j} \left[(v + \sigma_\omega v_T) \frac{\partial \omega}{\partial x_j} \right] + 2(1 - F_1) \sigma_{\omega 2} \frac{1}{\omega} \frac{\partial k}{\partial x_i} \frac{\partial \omega}{\partial x_i} \quad (8)$$

Kinematic Eddy Viscosity

$$v_t = \frac{a_1 k}{\max(a_1 \omega, S F_2)} \quad (9)$$

where F_1 and F_2 are blending functions and P_k is the production limiter and it is expressed as:

$$F_1 = \tanh \left\{ \left\{ \min \left[\max \left(\frac{\sqrt{k}}{\beta^* \omega y}, \frac{500\nu}{y^2 \omega} \right), \frac{4\sigma_{\omega 2} k}{C D_{k\omega} y^2} \right] \right\}^4 \right\} \quad (10)$$

$$F_2 = \tanh \left[\left[\max \left(\frac{2\sqrt{k}}{\beta^* \omega y}, \frac{500\nu}{y^2 \omega} \right) \right]^2 \right] \quad (11)$$

$$P_k = \min \left(\tau_{ij} \frac{\partial U_i}{\partial x_j}, 10\beta^* k \omega \right) \quad (12)$$

$$C D_{k\omega} = \max \left(2\rho \sigma_{\omega 2} \frac{1}{\omega} \frac{\partial k}{\partial x_i} \frac{\partial \omega}{\partial x_i}, 10^{-10} \right) \quad (13)$$

where the values of the constants are

$$\beta^* = \frac{9}{100}, \sigma_{k1} = 0.85, \sigma_{k2} = 1, \sigma_{\omega 1} = 0.5, \sigma_{\omega 2} = 0.856.$$

3.3 Modeling Assumptions

The following assumptions are used in the present numerical study.

- (1) The fluid is considered as incompressible.
- (2) Apples are modeled as spherical object with 0.09 m diameter.
- (3) The heat of respiration of apples is considered to be 60 W/ton [12].

4 Boundary and Initial Conditions

The following boundary conditions are used in present study.

4.1 Inflow Boundary

For the inlet air through the package vents, inlet velocity and temperature are kept at 2 m/s and 2 °C, respectively.

4.2 Outflow Boundary

At the outlet of the duct, pressure outlet condition is specified, while a zero gradient condition is applied for all the velocity components.

4.3 Wall Boundaries

No-slip boundary condition is specified for duct, package, baffle, and apple surface. The walls of the duct are considered insulated walls.

4.4 Initial Conditions

Since the product is pre-cooled before storing it in the cold room, the initial temperature of the duct and apples is considered as 27 °C before calculations. The properties of the material used in the present study are given in Table 1.

5 Simulation Procedure and Mesh

The ANSYS FLUENT 2020 R1 solver is used in the present study. First order implicit method and second-order upwind scheme is used for transient formulation and spatial discretization, respectively. The tetrahedral hybrid mesh is generated with ANSYS mesher. At the product's surface, boundary layer mesh is used with Y^+ value less than 0.95. To obtain the appropriate grid size, grid size independence test is carried for four different grid sizes as given in Table 2. The change in wall shear stress at fruits surface for grid M3 and M4 is found to be negligible. Therefore, M3 is used

Table 1 Properties of the materials

Input material properties [2]		
Material	Property	Value (unit)
Air	Density	1.286 (kg m ⁻³)
	Dynamic viscosity	1.73 × 10 ⁻⁵ (Pa * s)
	Specific heat capacity	1004.8 (Jkg ⁻¹ K ⁻¹)
	Thermal conductivity	0.242 (Wm ⁻¹ K ⁻¹)
Apple	Density	837.22 (kg m ⁻³)
	Diameter	0.009 (m)
	Specific heat	3821.96 (Jkg ⁻¹ K ⁻¹)
	Thermal conductivity	0.4508 (Wm ⁻¹ K ⁻¹)
Package material	Density	220 (kg m ⁻³)
	Specific heat	1700 (Jkg ⁻¹ K ⁻¹)
	Thermal conductivity	0.05 (Wm ⁻¹ K ⁻¹)

in further numerical study. The enlarged view (near the wall boundary) with the full mesh of the duct is shown in Fig. 3.

Table 2 Grid size independence test

Grid name	Total number of grid elements	Wall shear stress on the fruit surface (Pa)	Change in %
M1	731,914	2.72 × 10 ⁻³	—
M2	1,231,356	2.79 × 10 ⁻³	2.50
M3	2,510,842	2.83 × 10 ⁻³	1.41
M4	3,914,535	2.84 × 10 ⁻³	0.35

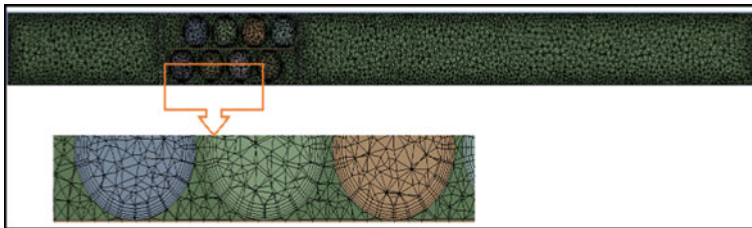


Fig. 3 Full and enlarged view of mesh

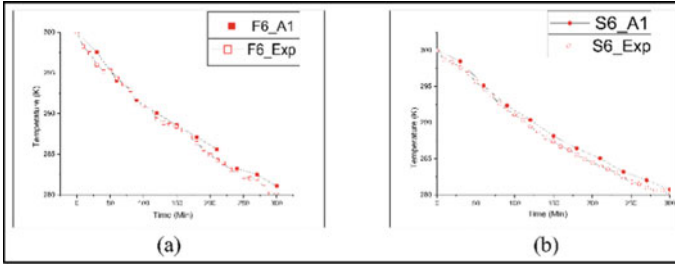


Fig. 4 Validation of the numerical model with the experimental results

6 Validation of the CFD Model

The present CFD model is validated with the experimental results from the published research [2]. The temperature of the product with respect to time is plotted for two different locations (F6 and S6) in plane 1 and plane 2. The numerical results show a good agreement with the experimental results, as shown in Fig. 4.

7 Results and Discussion

In the present study, the cooling profile for three different package designs is numerically simulated. A time step of 60 s with 20 iterations per time step is used for transient simulation. To observe the effect of different vent positions on the package, two horizontal planes and two product locations (one in each plane) are identified. The planes and locations are shown in Fig. 5a, b, respectively.

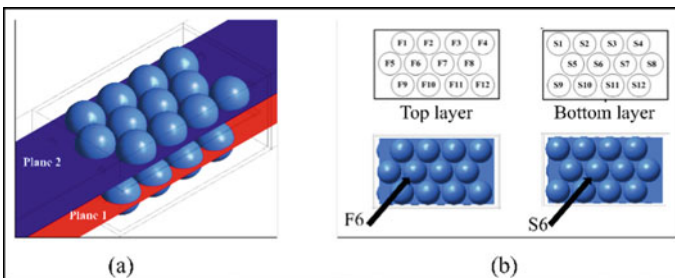


Fig. 5 **a** Location of the planes for temperature and velocity profile and **b** locations of temperature measurement

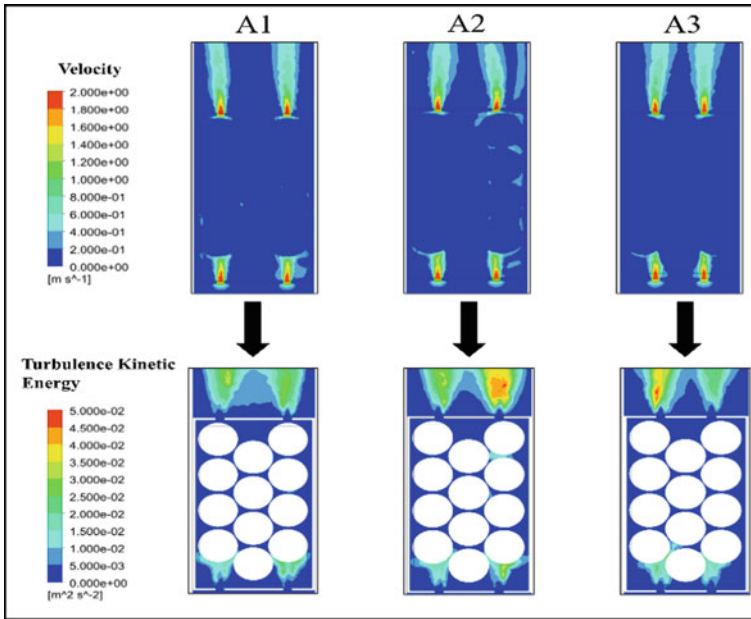


Fig. 6 Velocity contour and turbulence kinetic energy at plane 1 after 300 min of cooling time

7.1 Temperature and Velocity Distribution

The air velocity distribution and associated turbulence kinetic energy is shown in Fig. 6 at plane 1 after 300 min of cooling time. An insignificant difference in the velocity distribution is observed among all three designs (A1, A2, and A3) because of the compact stacking of the apples inside the package. The temperature contours after 300 min of cooling time are plotted at plane 1 and plane 2 for all three designs and shown in Fig. 7. It is seen from the Fig. 7 that the temperature of the product at the rear part of the package is cooled down to a lower temperature in A2 and A3 when compared with A1. A maximum cooling is reported in design A3 among other two designs.

7.2 Temperature Inhomogeneity

Dispersion degree of dimensionless temperature parameter Y_i is used to define the temperature inhomogeneity at any plane. This dimensionless temperature parameter has been reported in previous studies [5, 13].

$$Y_i = T_{i,t} - T_a / T_{in} - T_a \tag{14}$$

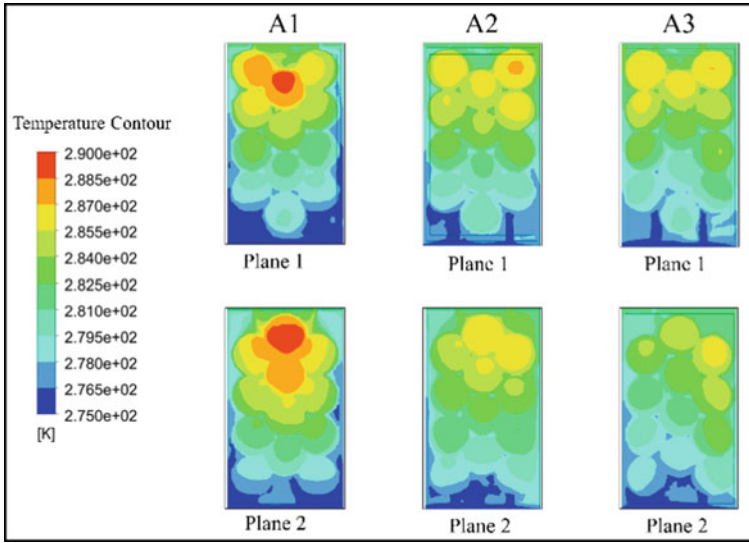


Fig. 7 Temperature contours at plane 1 and plane 2 after 300 min of cooling time

where

- Y_i is the dimensionless temperature parameter,
- $T_{i,t}$ is the temperature of the product at time t ,
- T_a is the air temperature,
- T_{in} is the initial temperature of the product.

The above dimensionless parameter is used to calculate the temperature inhomogeneity as:

$$\sigma = \max \left\{ Y_i - \frac{1}{n} \sum_{i=1}^n Y_i \right\} - \min \left\{ Y_i - \frac{1}{n} \sum_{i=1}^n Y_i \right\} \tag{15}$$

The variation of product temperature with time is plotted in Fig. 8a and temperature inhomogeneity in three designs is shown in Fig. 8b. It is observed that changing the positions of the vent hole on the package changes the temperature inhomogeneity significantly. The maximum temperature inhomogeneity is observed in package design A1, while it is minimum for design A3. After 300 min of cooling time, the temperature inhomogeneity is found to be reduced by 25.8% in design A3 compared with design A1.

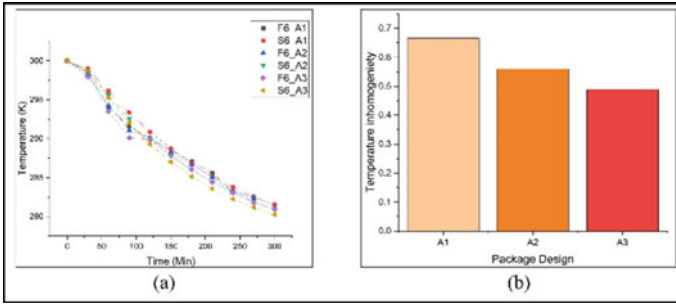


Fig. 8 a Temperature profile at F6 and S6 location for all the designs with respect to the time and b temperature inhomogeneity in all the three package designs after 300 min of cooling time

8 Conclusion

The temperature distribution inside the package filled with apples with different vent positions is investigated numerically. The obtained results of design A1 show good agreement with the experimental results. It is found that temperature inhomogeneity inside the package is dependent on the vent position and it reduces in design A3. After 300 min of cooling time, the temperature inhomogeneity is reduced up to 25.8% for A3 compared with existing package design A1.

Nomenclature

- ρ_f Density of fluid [kg m^{-3}]
- λ_f Thermal conductivity of fluid [$\text{Wm}^{-1}\text{K}^{-1}$]
- C_{p_f} Specific heat of fluid [$\text{Jkg}^{-1}\text{K}^{-1}$]
- ν_t Kinematic eddy viscosity [m^2s^{-1}]
- k Turbulence kinetic energy [m^2s^{-2}]
- λ_{eff} Effective turbulent thermal conductivity [$\text{Wm}^{-1}\text{K}^{-1}$]
- Pr_t Turbulent Prandtl number
- Y_i Dimensionless temperature parameter
- $T_{i,t}$ Temperature of the product at time t [$^{\circ}\text{C}$]
- T_a Temperature of air [$^{\circ}\text{C}$]
- T_{in} Initial temperature of the product [$^{\circ}\text{C}$]
- σ Temperature inhomogeneity

References

1. Duan Y, Wang GB, Fawole OA, Verboven P, Zhang XR, Wu D, Opara UL, Nicolai B, Chen K (2020) Postharvest precooling of fruit and vegetables: a review. *Trends Food Sci Technol* 100:278–291
2. Han JW, Zhao CJ, Yang XT, Qian JP, Fan BL (2015) Computational modeling of airflow and heat transfer in a vented box during cooling: optimal package design. *Appl Therm Eng* 91:883–893
3. Han JW, Qian JP, Zhao CJ, Yang XT, Fan BL (2017) Mathematical modelling of cooling efficiency of ventilated packaging: integral performance evaluation. *Int J Heat Mass Transf* 111:386–397
4. Wang D, Lai Y, Zhao H, Jia B, Wang Q, Yang X (2019) Numerical and experimental investigation on forced-air cooling of commercial packaged strawberries. *Int J Food Eng* 15(7):1–14
5. Han JW, Zhao CJ, Qian JP, Ruiz-Garcia L, Zhang X (2018) Numerical modeling of forced-air cooling of palletized apple: integral evaluation of cooling efficiency. *Int J Refrig* 89:131–141
6. Gruyters W, Defraeye T, Verboven P, Berry T, Ambaw A, Opara UL, Nicolai B (2019) Reusable boxes for a beneficial apple cold chain: a precooling analysis. *Int J Refrig* 106:338–349
7. Gong YF, Cao Y, Zhang XR (2021) Forced-air precooling of apples: airflow distribution and precooling effectiveness in relation to the gap width between tray edge and box wall. *Postharvest Biol Technol* 177:111523
8. Bishnoi R, Aharwal KR (2020) Experimental investigation of air flow field and cooling heterogeneity in a refrigerated room. *Eng Sci Technol Int J* 23(6):1434–1443
9. Bishnoi R, Aharwal KR (2021) Experimental evaluation of cooling characteristic, airflow distribution and mass transfer in a cold store. *J Food Process Eng* 44(2):1–11
10. Bishnoi R, Aharwal KR (2022) Experimental and theoretical analysis of mass transfer in a refrigerated food storage. *Heat Mass Transf*
11. Menter FR (1994) Two-equation eddy-viscosity turbulence models for engineering applications. *AIAA J* 32(8):1598–1605
12. Hoang HM, Duret S, Flick D, Laguerre O (2015) Preliminary study of airflow and heat transfer in a cold room filled with apple pallets: comparison between two modelling approaches and experimental results. *Appl Therm Eng* 76:367–381
13. Jia B (2021) The effect of alternating ventilation on forced air pre-cooling of cherries